MECSOL 2022 - Proceedings of the 8th International Symposium on Solid Mechanics
M.L. Bittencourt, J. Labaki, L.C.M. Vieira Jr. and E. Mesquita (Editors), Campinas SP, Brazil, October 17th to 19th, 2022

A Multiscale Hybrid-Mixed Method for Three-Dimensional Linear Elasticity

Nathan Shauer[1], Philippe R.B. Devloo[1], Sônia M. Gomes[2] and Jeferson W.D. Fernandes[1]

[1] LabMeC-FECAU-Universidade Estadual de Campinas, R. Josiah Willard Gibbs 85, Cidade Universitária, 13083-841, Campinas-SP, Brazil
[2] IMECC-Universidade Estadual de Campinas. R. Sergio Buarque de Holanda 651, Cidade Universitária, 13083-859, Campinas-SP, Brazil

Abstract. We consider two-scale hybrid-mixed finite element elasticity models using H(div)-conforming tensor approximations for the stress variable, whilst displacement and rotation fields represent multipliers to impose divergence and symmetry constraints. The discretization is based on general polyhedral meshes with flat faces (polytopes) in a global-local context. There are primary variables at the coarser level, solving normal stress trace (traction), piecewise defined over a partition of the mesh skeleton (facets), and piecewise polytope rigid motions. The fine details of the solution (secondary variables) are obtained by completely independent local Neumann problems in each polytope subdomain, the traction variable playing the role of boundary data. As compared to the traction accuracy, internal variables may be enriched with respect to internal mesh size, internal polynomial degree, or both. The polytope grid does not have to match across the facets, but a mild compatibility constraint is required. Stability and error estimates have been proved for the method using a variety of two-scale space configurations associated to known stable single-scale space settings for tetrahedral local sub-partitions. Enhanced accuracy rates for displacement and super-convergent divergence of the stress can be obtained. Stress, rotation, and stress symmetry errors keep the same accuracy order determined by the traction discretization. This analysis expands to three-dimensional elasticity problems the metodology recently published by the research group for polygonal elastic domains. Efficient computational implementation and numerical simulation results are presented to attest convergence properties of the method.
Keywords: Multiscale, Mixed Finite Elements, Linear Elasticity, Hybridization

INTRODUCTION

The importance of H(div)-conforming finite element (FE) spaces is well recognized for conservative mixed formulations of multiphysics systems in many fields. For instance, they are required for stable flux approximations in mixed methods for Darcy's flows, and for stress discretisations required in mixed stress formulations of linear elasticity problems (see, e.g., Boffi, Brezzi and Fortin, 2013). Our current interest is on H(div)-conforming FE spaces based general polyhedral meshes with flat faces (polytopes), allowing more refined discretization inside the elements than their traces over element interfaces, with respect to internal mesh size, internal polynomial degree, or both. This concept has been useful when dealing with the Multiscale Hybrid Mixed method (MHM) using mixed local solvers. For instance, in the work by Duran, et al. (2019) the MHM method was proposed for flows in porous media. Similar principle was extended by Devloo, et al. (2021) for two dimensional linear elasticity problems with weak enforcement of stress symmetry (and denoted by the acronym MHM-WS). The case of three-dimensional elastic bodies was analysed in the preprint by Devloo and Gomes (2021), but computational implementation was missing.

The MHM-WS method is the discrete version of a global-local hybrid formulation characterizing the exact solution, and it shares some typical properties of other MHM methods available in the literature (e.g. see Pereira (2019) and references therein): (i) given a polytope mesh $\mathcal{T} = \{\Omega_i\}$ of the computational region Ω, local problems over Ω_i are applied, under a divide-and-conquer principle; (ii) the inter-element connection is played by a trace variable (traction) defined over the facets of $\partial\Omega_i$ (mesh skeleton); (iii) there are global-local operators transferring information between the two levels of resolution: coarse and fine; (iv) the displacement is represented by a L^2-orthogonal decomposition in terms of a coarse component (piecewise rigid body motions over $\mathcal{T}$), and a fine-scale component; (v) the traction variable and the coarse displacement component are computed by a stable global system (static condensation); (vi) local independent problems are set to resolve small details by stable FE methods on $\Omega_i \in \mathcal{T}$, the traction variable playing the role of Neumann boundary data (favorable for parallelization). The bubble tensor components inside each subdomain, with vanishing normal traces on its

boundary, are allowed to be based in a more refined internal partition and/or using higher polynomial degree.

In this context, our main contribution is the implementation of the three-dimensional MHM-WS method in the computational framework NeoPZ[1], where tools for the construction of the required constrained H(div)-conforming spaces are available.

The text is organized as follows: firstly the model problem and the mixed formulation with weakly imposed stress symmetry are described. Next, the main aspects of the MHM-WS method for the model problem are summarized. Finaly, we comment about computational implementation and show results of a convergence verification test problem.

MODEL PROBLEM

Let $\Omega \subset \mathbb{R}^3$ be a connected polyhedral domain occupied by a linearly elastic body. Throughout the text, for a region $D \subseteq \Omega$, denote by $\underline{n}^D$ the external unitary normal to ∂D. Both scalar Hilbert spaces $L^2(D)$ and $H^s(D)$ have their usual meanings and norms. Associated vector or matrix valued spaces $L^2(D,\mathbb{E})$, and $H^s(D,\mathbb{E})$ shall be considered, where $\mathbb{E}$ will be either $\mathbb{R}^3$, $\mathbb{M} = \mathbb{R}^{3\times 3}$, symmetric $\mathbb{S} \subset \mathbb{M}$, or skew symmetric $\mathbb{K} \subset \mathbb{M}$ tensors. These spaces inherit the corresponding norms associated to the inner products in $L^2(D)$ and $H^s(D)$. The space $H(\mathrm{div},D)$ denotes the square-integrable vector functions, taking values in $\mathbb{R}^3$, for which the divergence is also square integrable. Similarly, we shall consider tensor functions in $H(\mathrm{div},D,\mathbb{M})$. These spaces inherit the corresponding norms associated to the inner products $(.,.)_D$ in $L^2(D)$, $L^2(D,\mathbb{R}^3)$, and $L^2(D,\mathbb{M})$. The notation $\langle\ ,\ \rangle_{\partial D}$ shall be used to define the duality pairing between the vector function spaces $H^{1/2}(\partial D,\mathbb{R}^3) = \left\{\underline{\mu} = \underline{u}|_{\partial D},\ \underline{u} \in H^1(D,\mathbb{R}^3)\right\}$, $H^{-1/2}(\partial D,\mathbb{R}^3) = \left\{\underline{\mu} = \underline{\underline{\tau}}\,\underline{n}^D,\ \underline{\underline{\tau}} \in H(\mathrm{div},D,\mathbb{M})\right\}$. Gradient ∇ and divergence $\nabla\cdot$ operators applied to scalar and vectorial fields have the usual meaning. For tensor fields $\underline{\underline{\tau}}$, the divergence is the vector field obtained by taking the divergence of each row $\underline{\tau}_i$: $\underline{\nabla}\cdot\underline{\underline{\tau}} = \begin{bmatrix}\nabla\cdot\underline{\tau}_1 & \nabla\cdot\underline{\tau}_2 & \nabla\cdot\underline{\tau}_3\end{bmatrix}$. The *Green's Formula* for $\underline{\underline{\tau}} \in H(\mathrm{div},D,\mathbb{M})$ and $\underline{v} \in H^1(D,\mathbb{R}^3)$ reads $(\underline{\nabla}\cdot\ \underline{\underline{\tau}},\underline{v})_D = -(\underline{\underline{\tau}},\underline{\underline{\varepsilon}}(\underline{v}))_D - (\underline{\underline{\tau}},\underline{\underline{\eta}}(\underline{v}))_D + <\underline{\underline{\tau}}\,\underline{n}^D,\underline{v}>_{\partial D}$, where, for a vector $\underline{u}$, the *deformation* and *rotation* tensors are defined by $\underline{\underline{\varepsilon}}(\underline{u}) = \frac{\nabla\underline{u}+\nabla\underline{u}^T}{2}$, and $\underline{\underline{\eta}}(\underline{u}) = \frac{\nabla\underline{u}-\nabla\underline{u}^T}{2}$. For a vector $\underline{v} = \begin{bmatrix}v_1 & v_2 & v_3\end{bmatrix}$ the curl operator gives $\underline{\nabla}\times\underline{v} = \begin{bmatrix}\partial_2 v_3 - \partial_3 v_2 & \partial_3 v_1 - \partial_1 v_3 & \partial_1 v_1 - \partial_2 v_1\end{bmatrix}$, and for a tensor with rows $\underline{\tau}_i$, $\underline{\underline{\nabla}}\times\underline{\underline{\tau}} = \begin{bmatrix}\underline{\nabla}\times\underline{\tau}_1 & \underline{\nabla}\times\underline{\tau}_2 & \underline{\nabla}\times\underline{\tau}_3\end{bmatrix}$.

The equations of static elasticity in Hellinger-Reissner form determine fields for the stress $\underline{\underline{\sigma}}$ and the displacement $\underline{u}$ satisfying the equilibrium and constitutive equations $-\underline{\nabla}\cdot\underline{\underline{\sigma}} = \underline{f}$, $\underline{\underline{\sigma}} = \underline{\underline{A}}\,\underline{\underline{\varepsilon}}(\underline{u})$, in Ω, and boundary conditions $\underline{u} = \underline{g}$, on $\partial\Omega_D$, $\underline{\underline{\sigma}}\,\underline{\eta} = 0$, on $\partial\Omega_N$. The functions $\underline{g} \in H^{\frac{1}{2}}(\partial\Omega_D)$ and $\underline{f} \in L^2(\Omega,\mathbb{R}^3)$ are given Dirichlet boundary data and body force, $\partial\Omega_D$ having positive measure. The material properties are described by the rigidity tensor $\underline{\underline{A}} = \underline{\underline{A}}(\underline{x})$, which is a self-adjoint, bounded, and uniformly positive definite linear operator acting from $\mathbb{S}$ to $\mathbb{S}$. We assume that $\underline{\underline{A}}$ can be extended to an operator from $\mathbb{M}$ to $\mathbb{M}$ with the same properties. In particular, in the case of homogeneous and isotropic body, $\underline{\underline{A}}\,\underline{\underline{\varepsilon}} = 2\mu\underline{\underline{\varepsilon}} + \lambda\,\mathrm{tr}(\underline{\underline{\varepsilon}})\underline{\underline{I}}$, λ and μ being the Lamé parameters, and $\underline{\underline{I}}$ the 3×3 identity matrix. This elasticity model problem admits an equivalent expression, without assuming stress symmetry a priori, by replacing the original constitutive equation $\underline{\underline{\sigma}} = \underline{\underline{A}}\,\underline{\underline{\varepsilon}}(\underline{u})$ by $\underline{\underline{A}}^{-1}\underline{\underline{\sigma}} = \nabla\underline{u} - \underline{\underline{\eta}}(\underline{u})$, using the relation $\underline{\underline{\varepsilon}}(\underline{u}) = \nabla\underline{u} - \underline{\underline{\eta}}(\underline{u})$. A new equation $\underline{\underline{\sigma}} - \underline{\underline{\sigma}}^T = 0$ enforces the desired stress symmetry, and a new rotation variable $\underline{\underline{q}} = \underline{\underline{\eta}}(\underline{u}) \in L^2(\Omega,\mathbb{K})$ is introduced to act as a Lagrange multiplier to enforce the symmetry constraint of the stress tensor.

Under this point of view, the mixed formulation with weakly imposed stress symmetry searches for $(\underline{\underline{\sigma}},\underline{u},\underline{\underline{q}}) \in H(\mathrm{div},\Omega,\mathbb{M}) \times L^2(\Omega,\mathbb{R}^d) \times L^2(\Omega,\mathbb{K})$ satisfying $\underline{\underline{\sigma}}\,\underline{n}^\Omega|_{\Gamma_N} = 0$, and

$$(\underline{\underline{A}}^{-1}\,\underline{\underline{\sigma}},\underline{\underline{\tau}}) + (\underline{u},\underline{\nabla}\cdot\underline{\underline{\tau}}) + (\underline{\underline{q}},\underline{\underline{\tau}}) = \langle\underline{\underline{\tau}}\,\underline{n}^\Omega,\underline{g}\rangle_{\partial\Omega_D}, \quad \forall\underline{\underline{\tau}} \in H(\mathrm{div},\Omega,\mathbb{M}), \tag{1}$$

$$-(\underline{\nabla}\cdot\underline{\underline{\sigma}},\underline{v}) = (\underline{f},\underline{v}), \qquad \forall\underline{v} \in L^2(\Omega,\mathbb{R}^3), \tag{2}$$

$$(\underline{\underline{\sigma}},\underline{\underline{\beta}}) = 0, \qquad \forall\underline{\underline{\beta}} \in L^2(\Omega,\mathbb{K}). \tag{3}$$

This kind of variational formulation typically appear in minimization problems with constraints (e.g., see Brezzi, 1974). For this model problem there is a constraint for the realization of the divergence equation (2), and

[1] NeoPZ open source platform: http://github.com/labmec/neopz

displacement plays the role of the corresponding Lagrange multiplier. The other multiplier is $\underline{\underline{q}}$, used for the weak enforcement of stress symmetry in (3). According to Brezzi's theory, the variational formulation (1)-(3) is well posed, but for its FE discretizations the approximations spaces of each field cannot be chosen independently one from the other, i.e., they should be compatible, meaning that some stability (inf-sup) conditions are mandatory.

TWO-SCALE STRESS ELASTICITY MODEL WITH REDUCED SYMMETRY

Our focus is on discrete FE models seaching for $(\underline{\underline{\tilde{\sigma}}},\tilde{\underline{u}},\underline{\underline{\tilde{q}}}) \in \mathscr{S}_\gamma, \times \mathscr{U}_{\gamma_{in}}, \times \mathscr{Q}_{\gamma_{in}}$ satisfying $\underline{\underline{\sigma}}_\gamma \underline{n}^\Omega|_{\Omega_N} = 0$,

$$(\underline{\underline{A}}^{-1}\,\underline{\underline{\tilde{\sigma}}},\underline{\underline{\tau}}) + (\tilde{\underline{u}},\underline{\nabla}\cdot\underline{\underline{\tau}}) + (\underline{\underline{\tilde{q}}},\underline{\underline{\tau}}) = \langle \underline{\underline{\tau}}\,\underline{n}^\Omega, \underline{g}\rangle_{\partial\Omega_D}, \quad \forall \underline{\underline{\tau}} \in, \tag{4}$$

$$-(\underline{\nabla}\cdot\underline{\underline{\tilde{\sigma}}},\underline{v}) = (\underline{f},\underline{v}), \qquad \forall \underline{v} \in \mathscr{U}_{\gamma_{in}}, \tag{5}$$

$$(\underline{\underline{\tilde{\sigma}}},\underline{\underline{\beta}}) = 0, \qquad \forall \underline{\underline{\beta}} \in \mathscr{Q}_{\gamma_{in}}. \tag{6}$$

based on two-scale FE space settings

$$\mathcal{E}_\gamma = \mathscr{S}_\gamma \times \mathscr{U}_{\gamma_{in}} \times \mathscr{Q}_{\gamma_{in}} \subset H(\mathrm{div},\Omega,\mathbb{M}) \times L^2(\Omega,\mathbb{R}^3) \times L^2(\Omega,\mathbb{K}.)$$

They are associated to a partition $\mathcal{T} = \{\Omega_i\}$ of the computational domain Ω by subdomains Ω_i, which may have one of the usual element geometry, but the focus is on more general polyhedral subdomains with flat faces. The two-scale frameworks to be considered are indicated by the index $\gamma := (\gamma_{sk},\gamma_{in})$, where $\gamma_{sk} = (h_{sk},k_{sk})$ and $\gamma_{in} = (h_{in},k_{in})$ are used to differentiate discretization parameters for mesh widths and polynomial degrees at coarse and fine levels (but single-level cases $\gamma_{sk} = \gamma_{in}$ may be treated in the same context as well). Because of that, the method is identified by the acronym $\mathbf{MHM}-WS(\mathcal{E}_\gamma)$.

Geometry: The construction of the mesh hierarchy starts with a coarse conformal shape regular partition $\mathcal{T}_{h_{sk}}$ of Ω formed by the union of conformal sub-meshes $\mathcal{T}_{h_{sk}}^{\Omega_i}$ of the subdomains $\Omega_i \in \mathcal{T}$, all of them with characteristic mesh size h_{sk}. Refined internal partitions $\mathcal{T}_{h_{in}}^{\Omega_i}$ are obtained by the subdivision of $\mathcal{T}_{h_{sk}}^{\Omega_i}$. The examples discussed here are for affine tetrahedral elements $K \in \mathcal{T}_{h_{in}}^{\Omega_i}$, and for sake of simplicity, we restrict to the cases of uniform distributions of mesh resolution $h_{k_{in}}$. Associated to $\mathcal{T}$, let Γ be the mesh skeleton formed by the union of all facets in the boundaries $\partial\Omega_i$ and set a partition $\mathcal{T}^\Gamma$ of Γ by taking faces induced by $\mathcal{T}_{h_{sk}}$ over $\Gamma\setminus\partial\Omega$, and faces induced by $\mathcal{T}_{h_{in}}^{\Omega_i}$ over $\partial\Omega\cap\partial\Omega_i$. Thus, the characteristic sizes are h_{sk} for internal faces, and h_{in} otherwise. For neighboring subdomains Ω_i and Ω_j, the meshes $\mathcal{T}_{h_{in}}^{\Omega_i}$ and $\mathcal{T}_{h_{in}}^{\Omega_j}$ may be non-conformal over interfaces $\partial\Omega_i\cap\partial\Omega_j$. However, $\mathcal{T}^\Gamma$ and $\mathcal{T}_{h_{in}}^{\Omega_i}$ verify the *mesh consistency* property in the following sense: for a face $F \subset \partial\Omega_i$, the partition $\mathcal{T}^F$ inherited from $\mathcal{T}^\Gamma$ is coarser than (or equal to) the one induced on F by the internal mesh $\mathcal{T}_{h_{in}}^{\Omega_i}$. Figure 1 illustrates some aspects of the two-scale hierarchy of meshes. There is a macro-partition $\mathcal{T} = \{\Omega_1,\Omega_2\}$ formed by a hexahedron Ω_1 and a prism Ω_2 with quadrilateral interface F (left-image). Conformal tetrahedral partitions $\mathcal{T}_{h_{sk}}(\Omega_i)$, and the inherited skeleton partition $\mathcal{T}_{h_sk}^F$ are shonwn (center-image). At the second level, the mesh $\mathcal{T}_{h_{in}}^{\Omega_1}$ is obtained by the subdivision of one element $K \in \mathcal{T}_{h_{sk}}^{\Omega_1}$, and no mesh refinement in enforced ibn Ω_2 (right-image). Observe that, over $F = \Omega_1\cap\Omega_2$, the meshes of the two macro elements are not conformal but they satisfy the mesh consistency property.

Two-level FE settings $\mathcal{E}_\gamma$: The FE space settings are constructed by the following components:
FE pairs in Ω_i for stress and displacement: FE spaces $\mathscr{S}_{\gamma_{in}}(\Omega_i) = \left\{\underline{\underline{\tau}} \in H(\mathrm{div},\Omega_i,\mathbb{M});\ \underline{\underline{\tau}}|_K \in S(K,\mathbb{M}),\ \forall K \in \mathcal{T}_{h_{in}}^{\Omega_i}\right\}$ and $\mathscr{U}_{\gamma_{in}}(\Omega_i) = \left\{\underline{u} \in L^2(\Omega_i,\mathbb{R}^3);\ \underline{u}|_K \in U(K),\ \forall K \in \mathcal{T}_{h_{in}}^{\Omega_i}\right\}$ are constructed on top of the partitions $\mathcal{T}_{h_{in}}^{\Omega_i}$ in terms of FE spaces $S(K,\mathbb{M})$ and $U(K)$ for $K \in \mathcal{T}_{h_{in}}^{\Omega_i}$. The degree $k_{in} \geq k_{sk}$ refers to the polynomials associated to the normal traces $\underline{\underline{\tau}}\,\underline{n}^K|_{\partial K}$, $\underline{\underline{\tau}} \in S(K,\mathbb{M})$. A direct sum decomposition $\mathscr{S}_{\gamma_{in}}(\Omega_i) = \mathscr{S}^\partial_{\gamma_{in}}(\Omega_i) \oplus \mathring{\mathscr{S}}_{\gamma_{in}}(\Omega_i)$ holds, the tensors $\underline{\underline{\tau}} \in \mathring{\mathscr{S}}_{\gamma_{in}}(\Omega_i)$ having vanishing traces $\underline{\underline{\tau}}\,\underline{n}^{\Omega_j} = 0$ (bubble functions). Otherwise, $\underline{\underline{\tau}} \in \mathscr{S}^\partial_{\gamma_{in}}(\Omega_i)$ are called face functions. The FE pairs $\{\mathscr{S}_{\gamma_{in}}(\Omega_i),\mathscr{U}_{\gamma_{in}}(\Omega_i)\}$ are supposed to be divergence-consistent: $\underline{\nabla}\cdot\,\mathscr{S}_{\gamma_{in}}(\Omega_i) = \mathscr{U}_{\gamma_{in}}(\Omega_i)$. One natural way to cope with that is to define the FE spaces $S(K,\mathbb{M})$ and $U(K)$ by taking their rows from

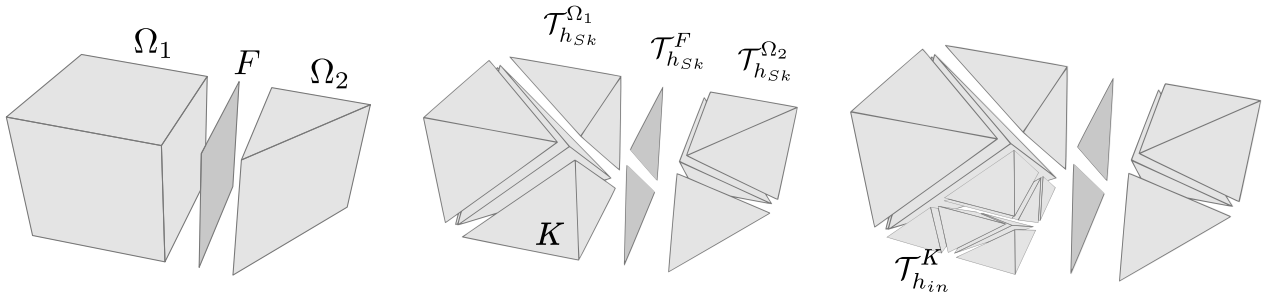

Figure 1: Diagram illustration of some aspects of a hierarchy of partitions and discretization parameters.

divergence-consistent FE pairs $V(K) \times P(K)$ that are usually applied for flux and potential approximations in mixed formulations of Poisson problems. For the current applications, we consider divergence-consistent FE pair of spaces of $BDFM_{k+1}$ type for tetrahedral elements K, with $S(K,\mathbb{M}) = \mathbb{P}_k(K,\mathbb{M}) \oplus \mathring{\mathbb{P}}_{k+1}(K,\mathbb{M})$ and $U(K) = \mathbb{P}_k(K)$.

Trace FE spaces: Let FE spaces $\Lambda_\gamma(\partial\Omega_i)$ piece-wisely defined over $\mathcal{T}^\Gamma|_{\partial\Omega_i}$ by vector polynomials of degree k_{sk} over the internal facets, and degree k_{in} over the ones in $\partial\Omega$. Thus, the important *trace consistency property* holds: the FE space of tracets $\underline{\underline{\tau}}\,\underline{n}|_{\partial\Omega_i}$, $\underline{\underline{\tau}} \in \mathscr{S}_{\gamma_{in}}(\Omega_i)$, contains $\Lambda_\gamma(\partial\Omega_i)$. In fact, the trace functions induced by $\mathscr{S}_{\gamma_{in}}(\Omega_i)$ over $\partial\Omega_i$ are piece-wisely defined by polynomials of degree $k_{in} \geq k_{sk}$ on top of elements which are obtained by the refinement of the mesh $\mathcal{T}^\Gamma|_{\partial\Omega_i}$ (due to the mesh consistency property).

Two-scale constrained tensor FE spaces: Under the above circumstances, we introduce two-scale constrained tensor FE spaces $\mathscr{S}_\gamma(\Omega_i) = \{\underline{\underline{\tau}} \in \mathscr{S}_{\gamma_{in}}(\Omega_i);\ \underline{\underline{\tau}}\,\underline{n}|_{\partial\Omega_i} \in \Lambda_\gamma(\partial\Omega_i)\}$. Due to the trace consistency property, these constrained tensor spaces are well defined. Moreover, the decomposition in terms of face and bubble components becomes $\mathscr{S}_\gamma(\Omega_i) = \mathscr{S}_\gamma^\partial(\Omega_i) \oplus \mathring{\mathscr{S}}_{\gamma_{in}}(\Omega_i)$. The face tensors in $\mathscr{S}_\gamma^\partial(\Omega_i)$, with normal traces over $\partial\Omega_i$ constrained to $\Lambda_\gamma(\partial\Omega_i)$, have coarser resolution γ_{sk} over $\partial\Omega_i \setminus \partial\Omega$. They are supported in the layer of elements $K \in \mathcal{T}_{h_{in}}^{\Omega_i}$ having a face included in $\partial\Omega_j$. The range of the divergence, which is determined by the bubble tensors, is not spoiled by doing the trace constraint operation. Thus, the divergence-consistency property is kept by the constrained tensors, so that $\underline{\nabla}\cdot\, \mathscr{S}_\gamma(\Omega_i) = \mathscr{U}_{\gamma_{in}}(\Omega_i)$.

Rotation FE spaces: $\mathscr{Q}_{\gamma_{in}}(\Omega_i) = \{\underline{\underline{q}} \in L^2(\Omega_i,\mathbb{K}); \underline{\underline{q}}|_K \in Q(K,\mathbb{K})\}$ can not be arbitrary. Stability also imposes a compatibility constraint on the FE pair $\mathscr{S}_\gamma(\Omega_i) \times \mathscr{Q}_{\gamma_{in}}(\Omega_i)$. The verification of this property is discussed in Devloo and Gomes (2021) for five cases of divergence-compatible FE pairs for tensor and displacement discretizations.

Finally, let $\mathcal{E}_\gamma = \mathscr{S}_\gamma \times \mathscr{U}_{\gamma_{in}} \times \mathscr{Q}_{\gamma_{in}} \subset H(\mathrm{div},\Omega,\mathbb{M}) \times L^2(\Omega,\mathbb{R}^3) \times L^2(\Omega;\mathbb{K})$ be the FE spaces whose restrictions to $\Omega_i \in \mathcal{T}$ are the local FE pairs $\mathscr{S}_\gamma(\Omega_i) \times \mathscr{U}_{\gamma_{in}}(\Omega_i) \times \mathscr{Q}_{\gamma_{in}}(\Omega_i)$. Similarly, $\Lambda_\gamma \subset L^2(\Gamma,\mathbb{R}^3)$ is composed by trace functions $\underline{\mu}$ whose restrictions on $\partial\Omega_i$ are in $\Lambda_\gamma(\partial\Omega_i)$.

Important properties

As discussed in Devloo and Gomes (2021), the positive properties of general stable FE mixed methods are held by the MHM-WS($\mathcal{E}_\gamma$) method. For instance, local conservation property is verified at the micro scale level, an essential property for ensuring local equilibrium. Furthermore, for $\underline{f} = 0$, the resulting tensor $\underline{\underline{\tilde{\sigma}}}$ is strongly divergence-free due to the divergence-compatibility condition. Moreover, classical tools adopted for mixed methods can be used for a unified stability and error analyses.

Implementation and simulation results presented in the next sections are for the particular case derived from the divergence-compatible $BDFM_{k+1}$ family for tetrahedral local partitions. Namely, taking $S(K,\mathbb{M}) = \mathbb{P}_k(K,\mathbb{M}) \oplus \mathring{\mathbb{P}}_{k+1}(K,\mathbb{M})$, $U(K) = \mathbb{P}_k(\hat{K},\mathbb{R}^d)$, and $Q(K,\mathbb{K}) = \mathbb{P}_k(K,\mathbb{K})$, the associated MHM-WS($\mathcal{E}_\gamma$) method is stable. Moreover, the following estimates hold under the elliptic regularity assumption, and assuming regular

enough exact fields $\underline{\underline{\sigma}}$, $\underline{u}$ and $\underline{q}$ (for the Sobolev norms to make sense).

$$2\|\underline{\underline{\sigma}}-\underline{\underline{\tilde{\sigma}}}\|_{\mathbf{L}^2(\Omega,\mathbb{M})}+\|\underline{q}-\underline{\tilde{q}}\|_{L^2(\Omega)} \lesssim h_{sk}^{k_{sk}+1}\|\underline{\underline{\sigma}}\|_{H^{k_{sk}+1}(\Omega,\mathbb{M})}+h_{in}^{k_{in}+1}\|\underline{q}\|_{H^{k_{in}+1}(\Omega)}, \tag{7}$$

$$\|\underline{\nabla}\cdot(\underline{\underline{\sigma}}-\underline{\underline{\tilde{\sigma}}})\|_{L^2(\Omega)} \lesssim h_{in}^{k_{in}+1}\|\underline{\nabla}\cdot\underline{\underline{\sigma}}\|_{H^{k_{in}+1}(\Omega)}, \tag{8}$$

$$\|\underline{u}-\underline{\tilde{u}}\|_{L^2(\Omega)} \lesssim h_{sk}^{k_{sk}+2}\|\underline{\underline{\sigma}}\|_{H^{k_{in}+1}(\Omega,\mathbb{M})}+h_{in}^{k_{in}+1}\|\underline{u}\|_{H^{k_{in}+1}(\Omega)}+h_{sk}h_{in}^{k_{in}+1}\|q\|_{H^{k_{in}+1}(\Omega)}. \tag{9}$$

The constants in these error estimates are independent of the Poisson ratio, a fact allowing to work with materials near the incompressible limit, avoiding the locking phenomena, which is one of main advantages of using stress mixed methods to solve linear elasticity.

GLOBAL-LOCAL SCHEMES

Implementation schemes for the MHM-WS($\mathcal{E}_\gamma$) method (4)-(6) explore the globa-local decomponsition $\mathscr{S}_\gamma = \mathscr{S}_\gamma^\partial \oplus \mathring{\mathscr{S}}_{\gamma_{in}}$ of the stress FE space and the L^2-orthogonal factorization $\mathscr{U}_{\gamma_{in}} = \mathscr{U}_{rm} \oplus \mathscr{U}_{\gamma_{in}}^\perp$ of the displacement FE space in terms of piecewise rigid-body modes, $\mathscr{U}_{rm} = \{\underline{u} \in L^2(\Omega,\mathbb{R}^d);\ \underline{u}_i = \underline{u}|_{\Omega_i} \in \mathscr{U}_{rm}(\Omega_i),\ \Omega_i \in \mathcal{T}\}$ and of its orthogonal complement $\mathscr{U}_{\gamma_{in}}^\perp$. Thus, the principle is to split stress and displacement variables by the corresponding components. That is,

$$\underline{\underline{\tilde{\sigma}}} = \underline{\underline{\tilde{\sigma}}}^\partial + \underline{\underline{\mathring{\tilde{\sigma}}}} \in \mathscr{S}_\gamma^\partial \oplus \mathring{\mathscr{S}}_{\gamma_{in}}, \quad \underline{\tilde{u}} = \underline{\tilde{u}}_{rm} + \underline{\tilde{u}}^\perp \in \mathscr{U}_{rm} \oplus \mathscr{U}_{\gamma_{in}}^\perp.$$

Given $(\underline{\underline{\tilde{\sigma}}}^\partial, \underline{\tilde{u}}_{rm})$ (primal variables), the remaining fields $(\underline{\underline{\mathring{\tilde{\sigma}}}}, \tilde{u}-\tilde{u}_{rm}, \tilde{q})$ (secondary variables) are piecewise obtained by solving the following local systems in the subregions Ω_i:

$$(\underline{\underline{A}}^{-1}\,\underline{\underline{\mathring{\tilde{\sigma}}}}, \underline{\underline{\mathring{\tau}}})_{\Omega_i} + (\tilde{u}, \underline{\nabla}\cdot\underline{\underline{\mathring{\tau}}})_{\Omega_i} + (\tilde{q}, \underline{\underline{\mathring{\tau}}})_{\Omega_i} + (\underline{\underline{A}}^{-1}\,\underline{\underline{\tilde{\sigma}}}^\partial, \underline{\underline{\mathring{\tau}}})_{\Omega_i} = 0, \quad \forall \underline{\underline{\mathring{\tau}}} \in \mathring{\mathscr{S}}_{\gamma_{in}}, \tag{10}$$

$$-(\underline{\nabla}\cdot\underline{\underline{\mathring{\tilde{\sigma}}}}, \underline{v})_{\Omega_i} - (\underline{\nabla}\cdot\underline{\underline{\tilde{\sigma}}}^\partial, \underline{v})_{\Omega_i} + (\tilde{\delta}, \underline{v})_{\Omega_i} = (\underline{f}, \underline{v})_{\Omega_i}, \quad \forall \underline{v} \in \mathscr{U}_{\gamma_{in}}, \tag{11}$$

$$(\underline{\underline{\mathring{\tilde{\sigma}}}}, \underline{\underline{\beta}})_{\Omega_i} + (\underline{\underline{\tilde{\sigma}}}^\partial, \underline{\underline{\beta}})_{\Omega_i} = 0, \quad \forall \underline{\underline{\beta}} \in \mathscr{Q}_{\gamma_{in}} \tag{12}$$

$$(\tilde{u}-\tilde{u}_{rm}, \underline{\kappa})_{\Omega_i} = 0 \quad \forall \underline{\kappa} \in \mathscr{U}_{rm} \tag{13}$$

$$(\underline{\underline{A}}^{-1}\,\underline{\underline{\tilde{\sigma}}}^\partial, \underline{\underline{\tau}}^\partial) + (\tilde{u}, \underline{\nabla}\cdot\underline{\underline{\tau}}^\partial) + (\underline{\underline{A}}^{-1}\underline{\underline{\mathring{\tilde{\sigma}}}}, \underline{\underline{\tau}}^\partial) + (\tilde{q}, \underline{\underline{\tau}}^\partial) = \langle \underline{\underline{\tau}}^\partial\, \underline{n}^\Omega, \underline{g}\rangle_{\partial\Omega_D}, \quad \forall \underline{\underline{\tau}}^\partial \in \mathscr{S}_\gamma^\partial, \tag{14}$$

$$(\underline{\delta}, \underline{v}_{rm}) = 0, \quad \forall \underline{v}_{rm} \in \mathscr{U}_{rm}. \tag{15}$$

The new auxiliary variable $\underline{\tilde{\delta}} \in \mathscr{U}_{rm}$ is introduced just to impose the solvability constraint $\tilde{u}-\tilde{u}_{rm} \in \mathscr{U}_{\gamma_{in}}^\perp$.

Within a local subregion Ω_i, the approximate fields can be expanded in terms of shape functions of the associated FE spaces:

- $\{\underline{\underline{\mathring{\tau}}}_\ell^i\}$ for $\mathring{\mathscr{S}}_{\gamma_{in}}(\Omega_i)$ and $\{\underline{\underline{\tau}}_\ell^{\partial i}\}$ for $\mathscr{S}_\gamma^\partial(\Omega_i)$.
- $\{\underline{v}_\ell^i\}$ for $\mathscr{U}_{\gamma_{in}}(\Omega_i)$, and $\{\underline{w}_\ell^i\}$ for $\mathscr{U}_{rm}(\Omega_i)$.
- $\{\underline{\underline{\beta}}_\ell^i\}$ for $\mathscr{Q}_{\gamma_{in}}^i$

Thus, locally in Ω_i the system of equations can be expressed in the following matrix form:

$$\left[\begin{array}{cccc|cc}
K_{0,0}^i & B_0^i & R_0^i & 0 & K_{0,1}^i & 0 \\
B_0^{iT} & 0 & 0 & C^i & B_1^{iT} & 0 \\
R_0^{iT} & 0 & 0 & 0 & R_1^{iT} & 0 \\
0 & C^{iT} & 0 & 0 & 0 & B_{rm}^i \\
\hline
K_{1,0}^i & B_1^i & R_1^i & 0 & K_{1,1}^i & 0 \\
0 & 0 & 0 & B_{rm}^{iT} & 0 & 0
\end{array}\right]
\left[\begin{array}{c}
\sigma_0^i \\ u^i \\ q^i \\ \delta^i \\ \hline \sigma_1^i \\ u_{rm}^i
\end{array}\right]
=
\left[\begin{array}{c}
0 \\ -F^i \\ 0 \\ 0 \\ \hline G_D^i \\ 0
\end{array}\right], \tag{16}$$

where the unknowns σ_0^i, u^i, q^i, δ^i, σ_1^i and u_{rm}^i represent the degrees of freedom (dof) of $\underline{\underline{\mathring{\tilde{\sigma}}}}$, $\underline{\tilde{u}}$, $\underline{\tilde{q}}$, $\underline{\tilde{\delta}}$, $\underline{\underline{\tilde{\sigma}}}^\partial$ and $\underline{\tilde{u}}_{rm}$ in Ω_i with respect to the corresponding shape functions. The associated block matrices are $K_{0,0}^i = [(\underline{\underline{A}}^{-1}\underline{\underline{\mathring{\tau}}}_\ell^i, \underline{\underline{\mathring{\tau}}}_j^i)_{\Omega_i}]$;

$B_0^i = [(\underline{v}_\ell^i, \nabla\cdot\mathring{\underline{\underline{\tau}}}_j^i)_{\Omega_i}]$, $R_0^i = [(\underline{\underline{\beta}}_\ell^i, \mathring{\underline{\underline{\tau}}}_j^i)_{\Omega_i}]$; $C^i = [-(\underline{w}_\ell^i, \underline{v}_j^i)_{\Omega_i}]$; $K_{11}^i = [(\underline{\underline{A}}^{-1}\underline{\underline{\tau}}_\ell^{\partial i}, \underline{\underline{\tau}}_j^{\partial i})]$, and $B_{rm}^i = [(\underline{w}_\ell, \underline{w}_j)]$. The terms on the right hand side are $G_D^i = [\langle \underline{\underline{\tau}}_j^{\partial i}\, \underline{n}^\Omega, \underline{g}\rangle_{\partial\Omega_D}]$, $F^i = [(\underline{f}, \underline{v}_j^i)]$.

System (16) can be expressed in the simplified notation

$$\begin{bmatrix} M_{00}^i & M_{01}^i \\ M_{10}^i & M_{11}^i \end{bmatrix} \begin{bmatrix} y_0^i \\ y_1^i \end{bmatrix} = \begin{bmatrix} r_0^i \\ r_1^i \end{bmatrix},$$

where $y_0^i = [\sigma_0^i, u^i, q^i, \delta^i]^T$, $y_1^i = [\sigma_1^i, u_{rm}^i]^T$, $r_0^i = [0, -F^i, 0, 0]^T$, $r_1^i = [G_D^i, 0]^T$,

$$M_{00}^i = \begin{bmatrix} K_{0,0}^i & B_0^i & R_0^i & 0 \\ B_0^{iT} & 0 & 0 & C^i \\ R_0^{iT} & 0 & 0 & 0 \\ 0 & C^{iT} & 0 & 0 \end{bmatrix}, \quad M_{01}^i = \begin{bmatrix} K_{0,1}^i & 0 \\ B_1^{iT} & 0 \\ R_1^{iT} & 0 \\ 0 & B_{rm}^i \end{bmatrix},$$

$$M_{10}^i = \begin{bmatrix} K_{1,0}^i & B_1^i & R_1^i & 0 \\ 0 & 0 & 0 & B_{rm,0}^{iT} \end{bmatrix}, \quad M_{11}^i = \begin{bmatrix} K_{11}^i & 0 \\ 0 & 0 \end{bmatrix}$$

Notice that M_{00}^i is non singular as the tangent matrix associated to well posed local Neumann boundary problems in Ω_i.

$$(\underline{\nabla}\cdot\tilde{T}^{\underline{\underline{\sigma}}}(\underline{\mu}), \underline{v})_{\Omega_i} = 0, \quad \forall \underline{v} \in \mathscr{U}_{\gamma_{in}}^{\perp}(\Omega_i), \tag{17}$$

$$(\underline{\underline{A}}^{-1}\,\tilde{T}^{\underline{\underline{\sigma}}}(\underline{\mu}), \underline{\underline{\tau}})_{\Omega_i} + (\tilde{T}^{\underline{u}}(\underline{\mu}), \underline{\nabla}\cdot\underline{\underline{\tau}})_{\Omega_i} + (\tilde{T}^{\underline{\underline{q}}}(\underline{\mu}), \underline{\underline{\tau}})_{\Omega_i} = 0, \quad \forall \underline{\underline{\tau}} \in \mathring{\mathscr{S}}_\gamma(\Omega_i), \tag{18}$$

$$(\tilde{T}^{\underline{\underline{\sigma}}}(\underline{\mu}), \underline{\underline{\eta}})_{\Omega_i} = 0, \quad \forall \underline{\underline{\eta}} \in \mathscr{Q}_{\gamma_{in}}(\Omega_i), \tag{19}$$

$$\tilde{T}^{\underline{\underline{\sigma}}}(\underline{\mu})\, \underline{n}|_{\partial\Omega_i} = \underline{\mu}|_{\partial\Omega_i}. \tag{20}$$

Thus, after usual static condensation procedure, we obtain the local matrix representation for the primary variables $K^i y_1^i = R^i$, where $K^i = M_{1,1}^i - M_{1,0}^i [M_{00}^i]^{-1} M_{01}^i$, and $R^i = r_1^i - M_{1,0}^i [M_{00}^i]^{-1} r_0^i$. Then, the assembly of the global system becomes $K y_1 = R$. After solving this global system for y_1, the secondary variables y_0^i are recovered by solving the local systems $M_{00}^i y_0^i = r_0^i - M_{01}^i y_1^i$.

The above-described algorithms are particularly attractive for a computational environment that offers the following tools for the construction of the restricted $H(\mathrm{div})$-conforming spaces:

- Hierarchic high order vector and scalar shape functions;
- A data structure allowing the identification of face and internal shape functions of different degree orders;
- A variety of refinement patterns and procedures for shape function restraints in two or three dimensions (as the ones usually adopted in adaptive *hp*-strategies);

This is the case of the object-oriented programming environment NeoPZ.

VERIFICATION TEST PROBLEM:

For the verification of the error estimates, we consider the model of simultaneous twisting and compression about the x_1-axis of the unit cube defined in $\Omega = [0,1]\times[0,1]\times[0,1]$ adopted in Khattatov & Yotov (2019). Taking Lamé parameters $\lambda = \mu = 100$, the displacement solution is

$$\underline{u} = \begin{bmatrix} -0.1(e^{x_1}-1)\sin(\pi x_1)\sin(\pi x_2) \\ -(e^{x_1}-1)(x_2 - \cos(\frac{\pi}{12})(x_2-0.5) + \sin(\frac{\pi}{12})(x_3-0.5) - 0.5) \\ -(e^{x_1}-1)(x_3 - \sin(\frac{\pi}{12})(x_2-0.5) - \cos(\frac{\pi}{12})(x_3-0.5) - 0.5) \end{bmatrix}$$

The meshes used for the simulations are illustrated in Figure 2 where the black lines represent edges of subdomains Ω_i and the yellow mesh represents the sub-meshes $\mathcal{T}_{h_{in}}^{\Omega_i}$ where one level uniform refinement is applied.

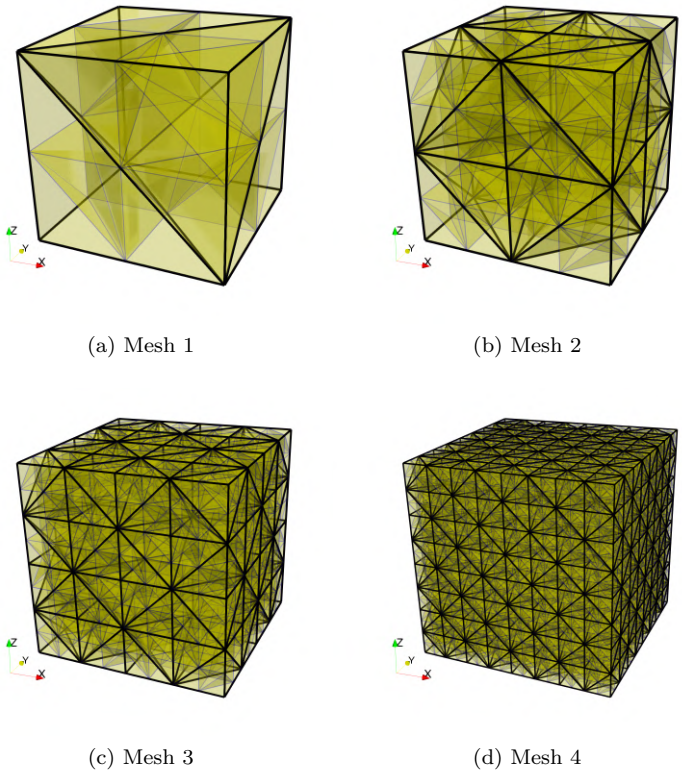

(a) Mesh 1 (b) Mesh 2

(c) Mesh 3 (d) Mesh 4

Figure 2: Finite Element meshes adopted for the error analyzes. The black lines illustrate the edges of subdomains Ω_i while the yellow mesh represents the sub-meshes $\mathcal{T}_{h_{in}}^{\Omega_i}$.

The simulations were carried with the $BDFM_{k+1}$ compatible finite element spaces previously described. In Figure 3, the computed errors $\|\underline{\underline{\sigma}}-\underline{\underline{\tilde{\sigma}}}\|_{\mathbf{L}^2(\Omega,\mathbb{M})}$, $\|\underline{\nabla}\cdot(\underline{\underline{\sigma}}-\underline{\underline{\tilde{\sigma}}})\|_{L^2(\Omega)}$, $\|\underline{u}-\underline{\tilde{u}}\|_{L^2(\Omega)}$ and $\|\underline{\underline{q}}-\underline{\underline{\tilde{q}}}\|_{L^2(\Omega}$ shown in estimates of equations (7), (8), and (9) are presented. The numerical values used to construct the plots are shown in Table 1, where it can be seen that the computed rates are in agreement with the predicted estimates presented in (7), (8) , and (9).

One of the main advantages of MHM is the possibility of applying static condensation from the sub-meshes onto the skeleton DoF's. Table 1 presents the number of DoF's of the full MHM problem and its corresponding condensed version, illustrating the potential computational time saving in the matrix decomposition step.

ACKNOWLEDGMENTS

We gratefully acknowledge the support of EPIC - Energy Production Innovation Center, hosted by the University of Campinas (Unicamp) and sponsored by Equinor Brazil and FAPESP - São Paulo Research Foundation (Process 2017/15736-3, N. Shauer FAPESP scholarship 2021/03791-5 and J. W. D. Fernandes scholarship 2021/02187-7). We acknowledge the support of ANP (Brazilian National Oil, Natural Gas and Biofuels Agency) through the R&D levy regulation. Acknowledgements are extended to the Center for Petroleum Studies (Cepetro), Faculty of Civil Engineering, Arquitecture and Urbanism (FECFAU) and Institute of Mathematics, Statistic and Scientific Computing (IMECC) of Unicamp. The authors P. R. B. Devloo and S. M. Gomes are grateful for the financial support from the Brazilian Research Council (CNPq), grants 305823/2017-5 and 306167/2017-4), respectively.

Table 1: Stress, Stress divergence, Displacement and Rotation errors in L^2-norm for $k = 1, 2$ and 3.

k	Mesh	h	DoF	DoF (cond.)	$\|\underline{\underline{\sigma}} - \underline{\underline{\tilde{\sigma}}}\|_{\mathbf{L}^2(\Omega,\mathbb{M})}$	$\|\underline{\nabla} \cdot (\underline{\underline{\sigma}} - \underline{\underline{\tilde{\sigma}}})\|_{L^2(\Omega)}$	$\|\underline{u} - \underline{\tilde{u}}\|_{L^2(\Omega)}$	$\|\underline{\underline{q}} - \underline{\underline{\tilde{q}}}\|_{L^2(\Omega}$
1	1	1	5,592	66	2.42E+01	1.07E+01	2.21E-02	6.32E+00
	2	0.5	44,088	744	6.77E+00	1.33E+00	2.65E-03	1.74E+00
	3	0.25	350,112	6,816	2.01E+00	1.69E-01	4.56E-04	4.85E-01
	4	0.125	2,790,528	57,984	5.46E-01	2.13E-02	6.78E-05	1.29E-01
Rate					1.88	2.99	2.87	1.91
2	1	1	11,484	102	5.35E+00	1.21E+00	2.28E-03	1.89E-02
	2	0.5	90,576	1,248	1.29E+00	1.24E-01	3.59E-04	5.80E-03
	3	0.25	719,424	11,712	1.85E-01	7.91E-03	2.70E-05	8.80E-04
	4	0.125	5,734,656	100,608	2.47E-02	4.98E-04	1.87E-06	1.22E-04
Rate					2.90	3.99	3.85	2.85
3	1	1	20,460	150	2.53E+00	3.22E-01	9.36E-04	9.50E-03
	2	0.5	161,520	1,920	1.83E-01	9.72E-03	3.42E-05	7.30E-04
	3	0.25	1,283,520	18,240	1.45E-02	3.09E-04	1.58E-06	6.56E-05
	4	0.125	10,233,600	157,440	9.67E-04	9.90E-06	5.52E-08	4.54E-06
Rate					3.90	4.96	4.84	3.85

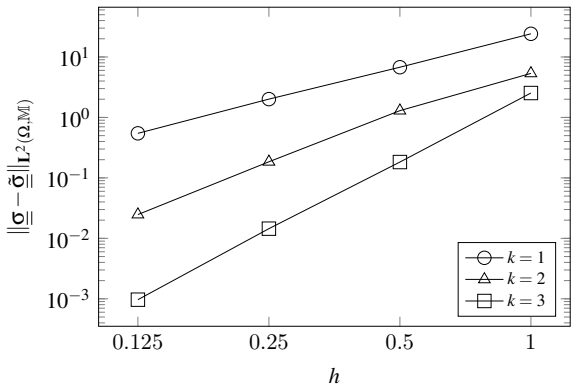

(a) Stress error.

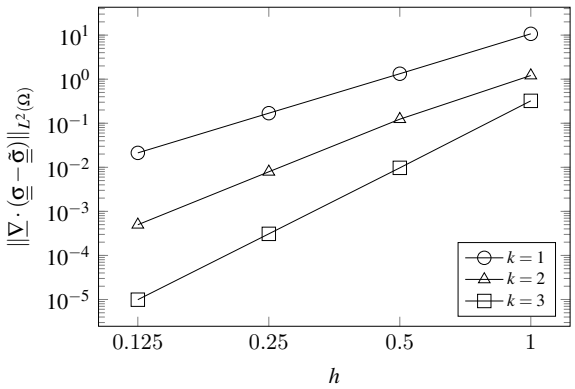

(b) Stress divergence error.

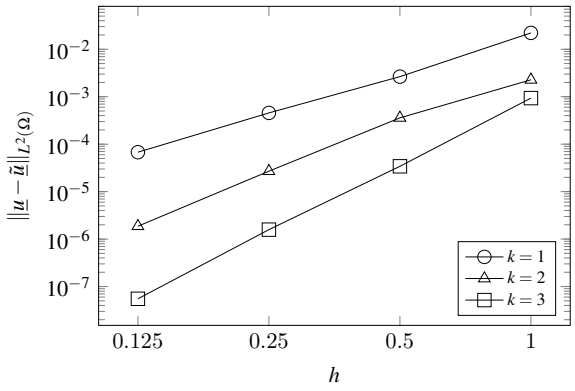

(c) Displacement error.

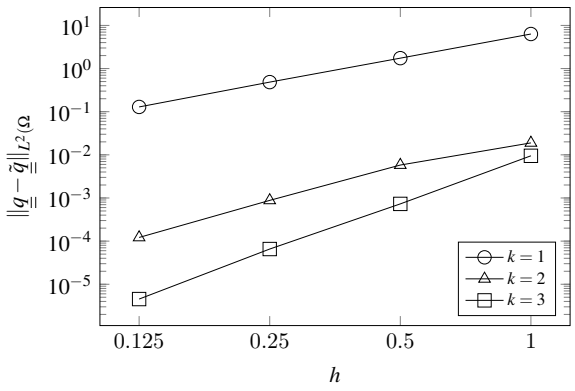

(d) Rotation error.

Figure 3: Plots of Stress, Stress divergence, Displacement and Rotation errors in L^2-norm for $k = 1, 2$ and 3.

REFERENCES

Brezzi, F. 1974, "On the existence, uniqueness and approximation of saddle-point problems arising from Lagrangian multipliers", R.A.I.R.O Anal. Numé r. Vol. 2, pp. 129-151.

Boffi, D., Brezzi, F., and Fortin, F. M., 2013, "Mixed Finite Element Methods and Applications", Springer.

Devloo, P. R. B., Farias, A. M., Gomes, S. M, Pereira, W., dos Santos, A. J. B, and Valentin, F., 2021, "New H(div)-conforming multiscale hybrid-mixed methods for the elasticity problem on polygonal meshes", ESAIM: Math. Model. Numer. Anal. Vol. 55, pp. 1005-1037.

Devloo, P. R. B., Gomes, S. M., 2021, Hybrid-mixed finite elements on polytopal meshes for two-scale elasticity models with relaxed symmetry, hal-03166493.

Durán, O., Devloo, P. R. B., Gomes, S. M., and Valentin, F., 2019, "A multiscale hybrid method for Darcy's problems using mixed finite element local solvers", Comput. Meth. Appl. Mech. Engr. Vol.354, pp. 213-244.

Khattatov, E. and Yotov, I., 2019, "Domain decomposition and multiscale mortar mixed finite elements methods for linear elasticity with weak stress symmetry", Math. Model. Numer. Anal. Vol. 53, pp. 2081 - 2108.

Pereira, W. S., 2019, "Multiscale Hybrid-Mixed Methods for Heterogeneous Elastic Models", Ph.D. thesis, LNCC, RJ, Brazil..

RESPONSIBILITY NOTICE

The authors are the only parties responsible for the printed material included in this paper.